Supporting Information

Zn-C$_x$N$_y$ nanoparticle arrays derived from metal-organic framework for ultralow-voltage hysteresis and stable Li metal anodes

Zilong Zhuang,[a] Chang Liu,[a] Yiyang Yan,[a] Pengcheng Ma,[b] and Daniel Q. Tan[a,*]

[a]Guangdong Technion Israel Institute of Technology, Shantou, 515063, China.

[b]China Machinery International Engineering Design & Research Institute Co., Ltd,

Changsha, 410021, China.
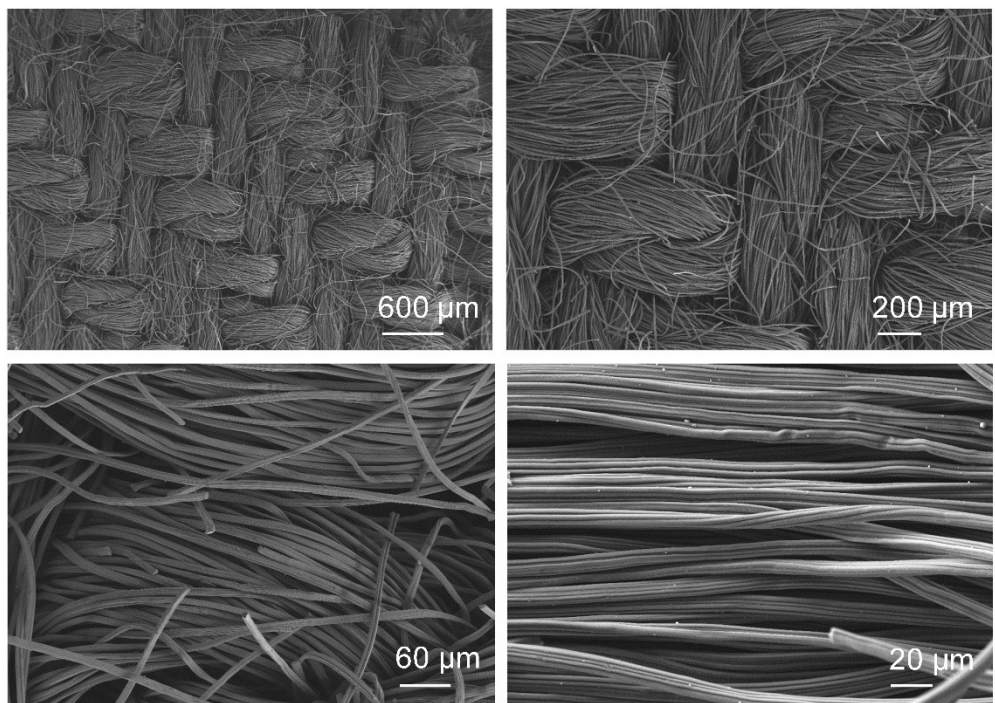
Fig. S1 SEM images of commercial carbon cloth (CC).
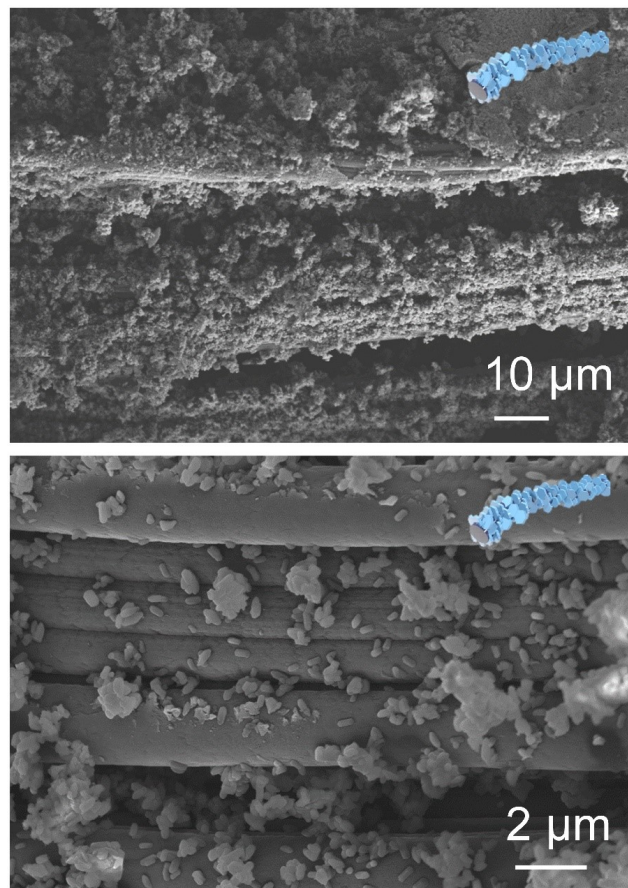
Fig. S2 SEM images of ZIF-8-CC, insets are the schematic figure of ZIF-8-CC.
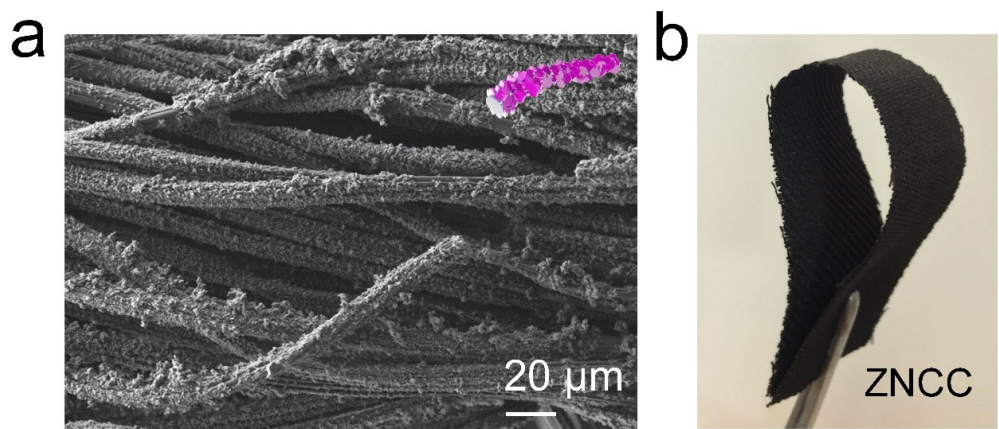
Fig. S3 (a) SEM image of ZNCC, inset is the schematic figure of ZIF-8-CC. (b) Photograph

of ZNCC, demonstrates its good flexibility.
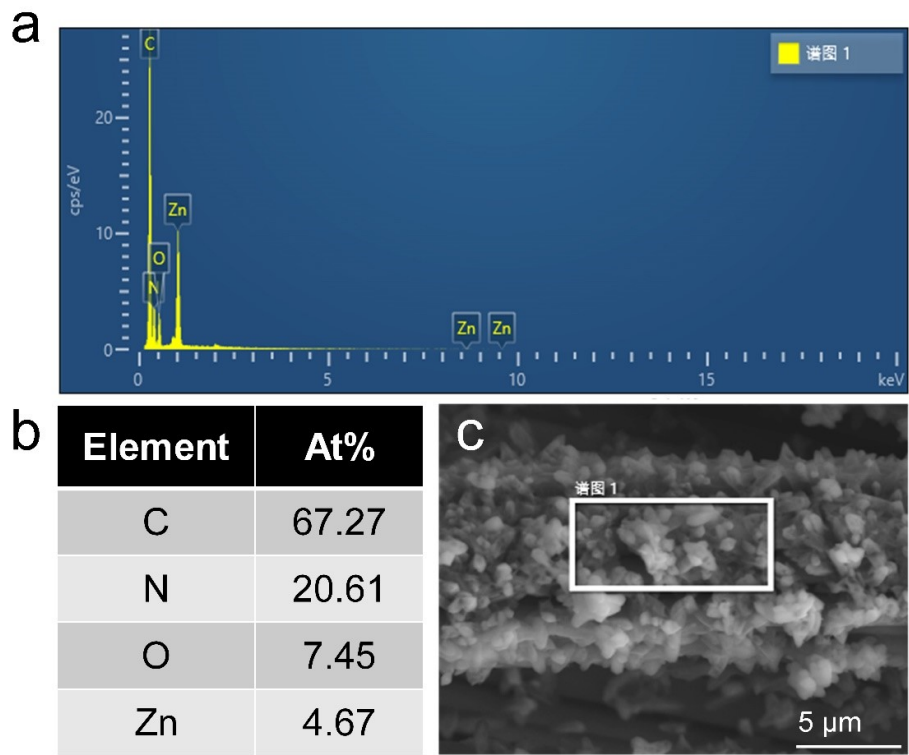
Fig. S4 (a) EDS spectrum of ZNCC. (b) Elements content and (c) SEM image of EDS test area.
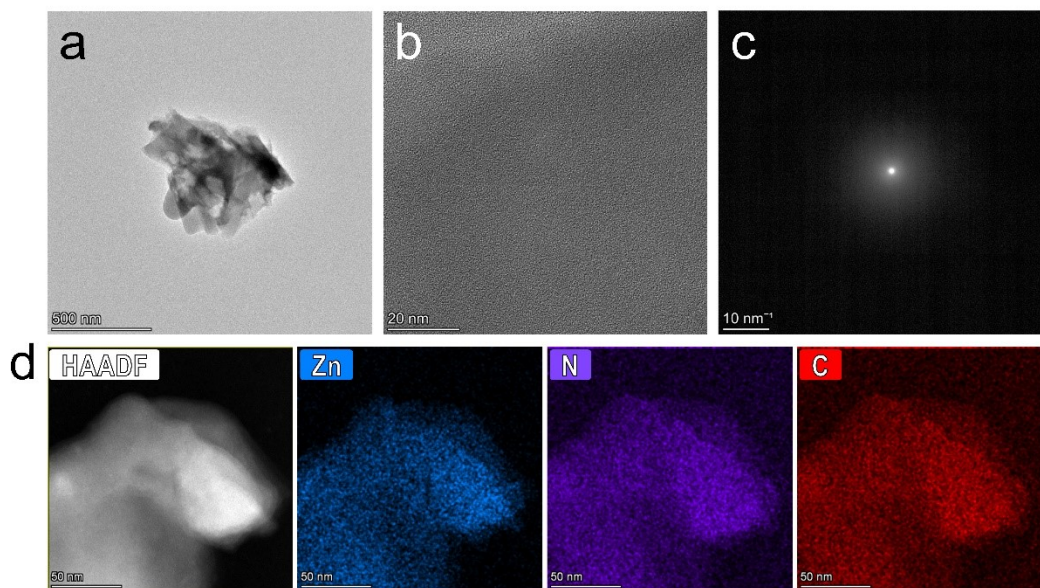
Fig. S5 (a,b) TEM images of ZNCC. (c) Selected area electron diffraction (SAED) pattern of ZNCC, demonstrates the C and Zn is amorphous state. (d) HAADF STEM image and EDS mapping of ZNCC.
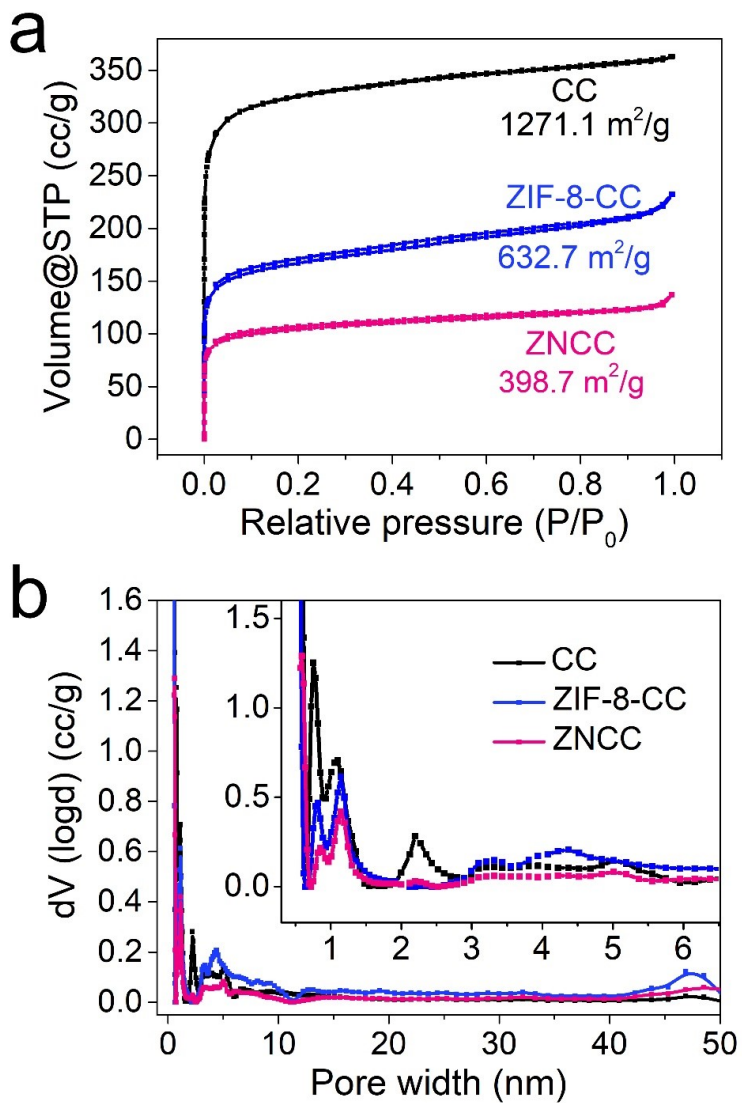
Fig. S6 (a) Dinitrogen absorption-desorption isothermal curve. (b) Pore size distributions from micropores to mesopores of CC, ZIF-8-CC and ZNCC.
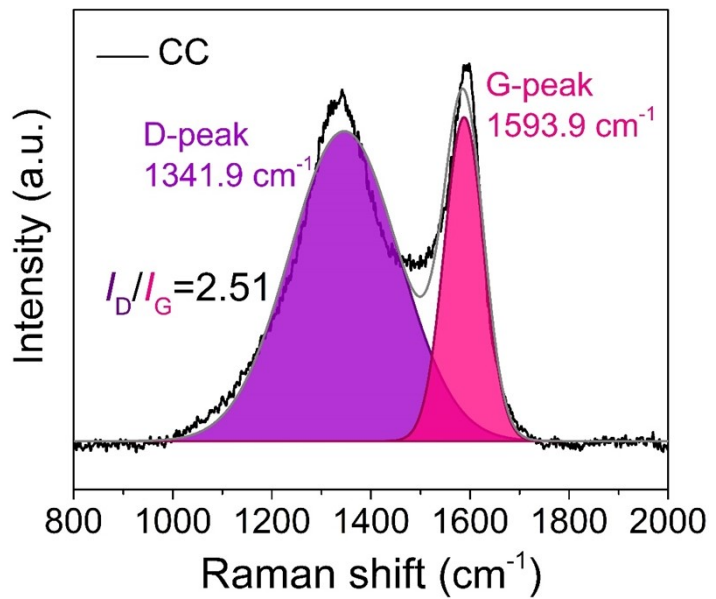
Fig. S7 Raman spectra of CC.
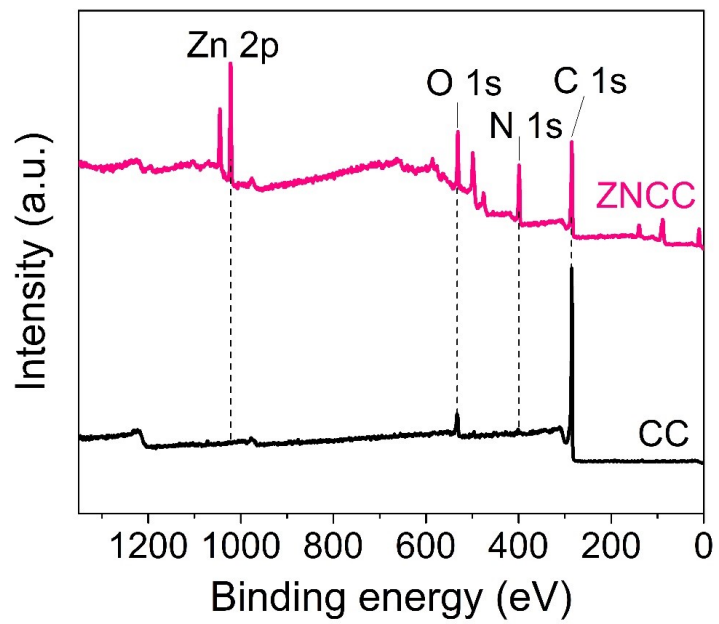
Fig. S8 XPS survey spectra of ZNCC and CC.
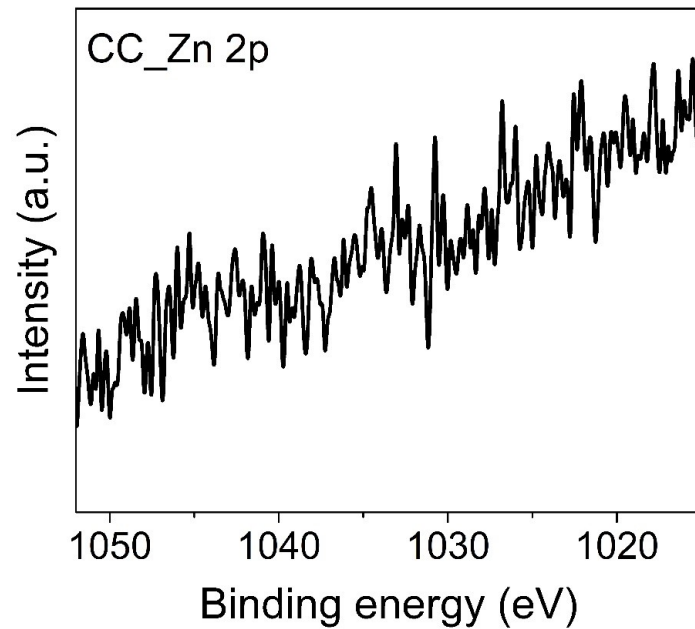
Fig. S9 Zn 2p XPS spectra of CC.
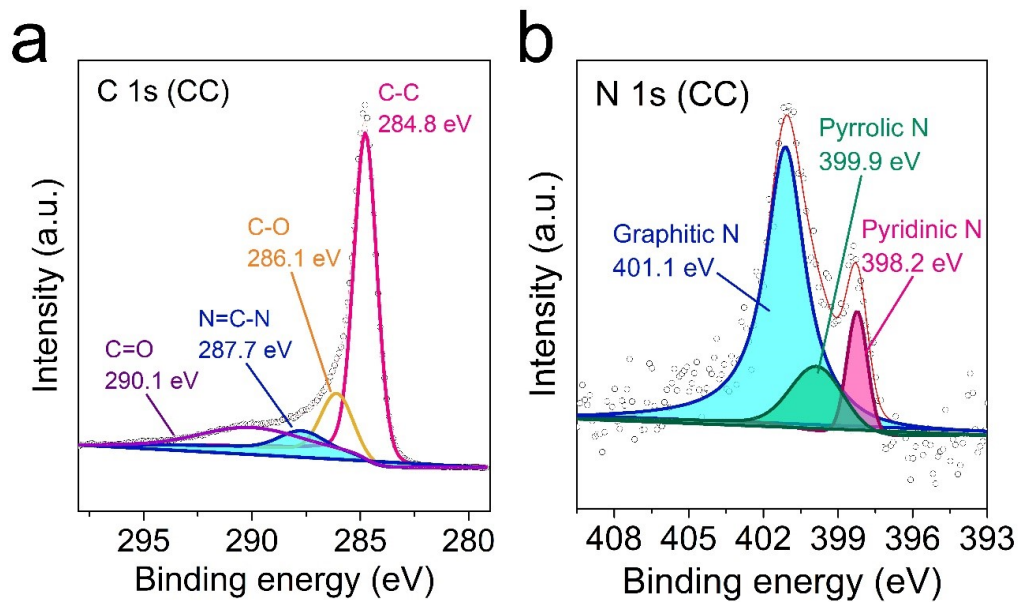
Fig. S10 (a) C 1s and (b) N 1s XPS spectra of CC.

Fig. S11 Photograph of ZNCC-Li.
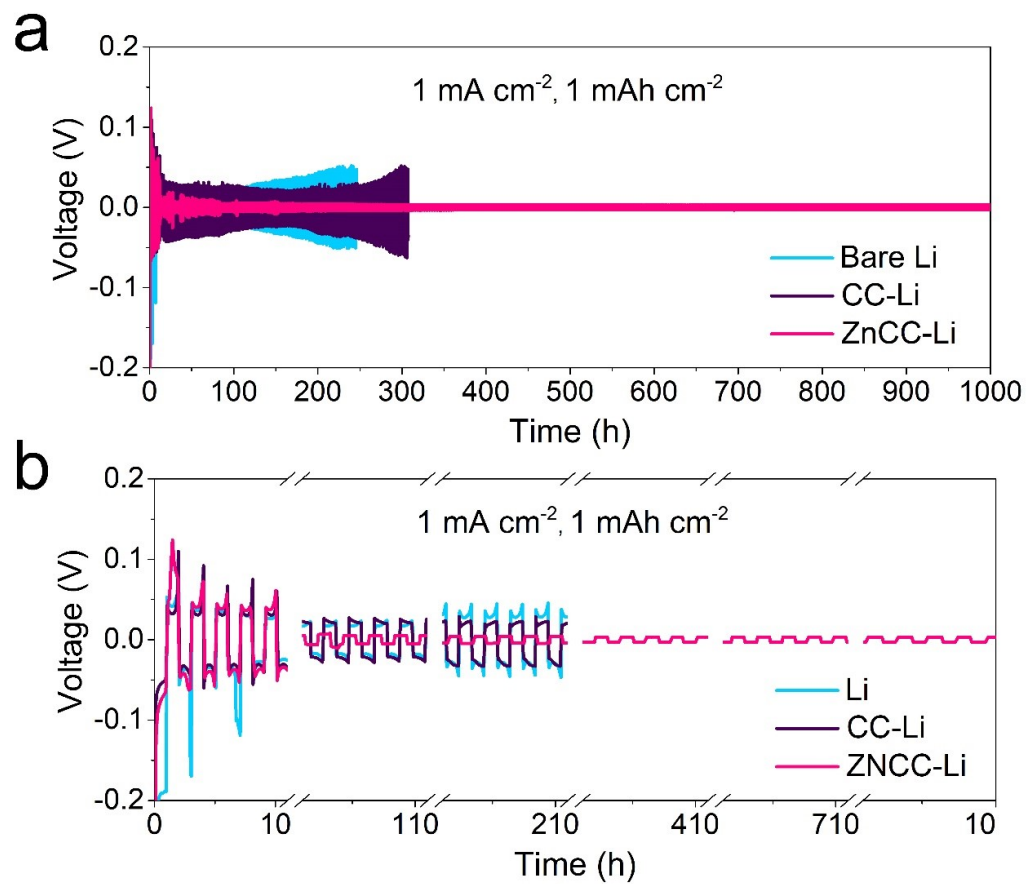
Fig. S12 (a) Voltage profiles of bare-Li, CC-Li and ZNCC-Li. (b) Enlarged voltage profiles at different cycles with a cycling capacity of 1 mA cm^{-2} to 1 mAh cm^{-2}.
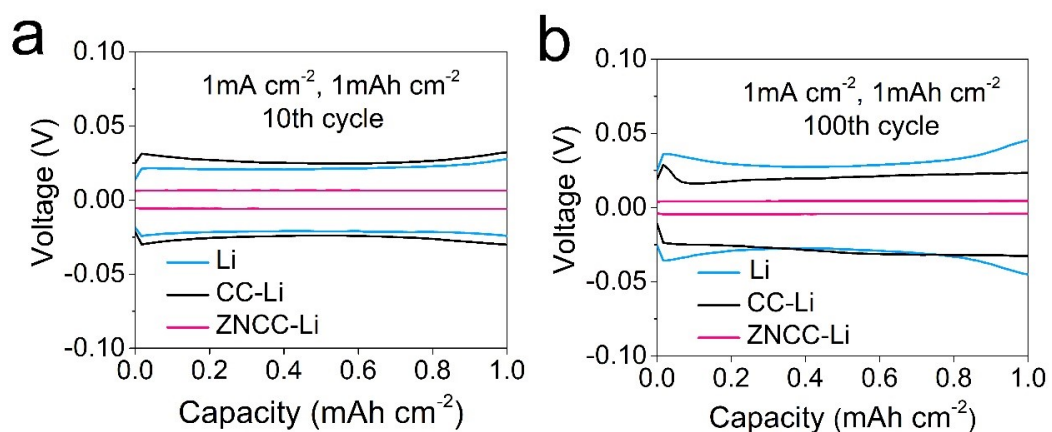
Fig. S13 Voltage profiles of bare-Li, CC-Li and ZNCC-Li at (a) 10th and (b) 100th cycle with a cycling capacity of 1 mA cm^{-2} to 1 mAh cm^{-2}.
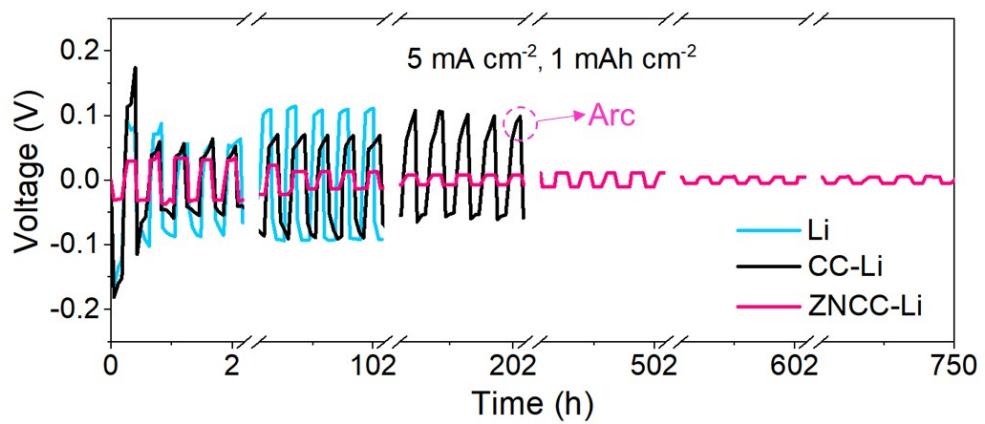
Fig. S14 Voltage profiles of bare-Li, CC-Li and ZNCC-Li at different cycle with a cycling

capacity of 5 mA cm^{-2} to 1 mAh cm^{-2}.
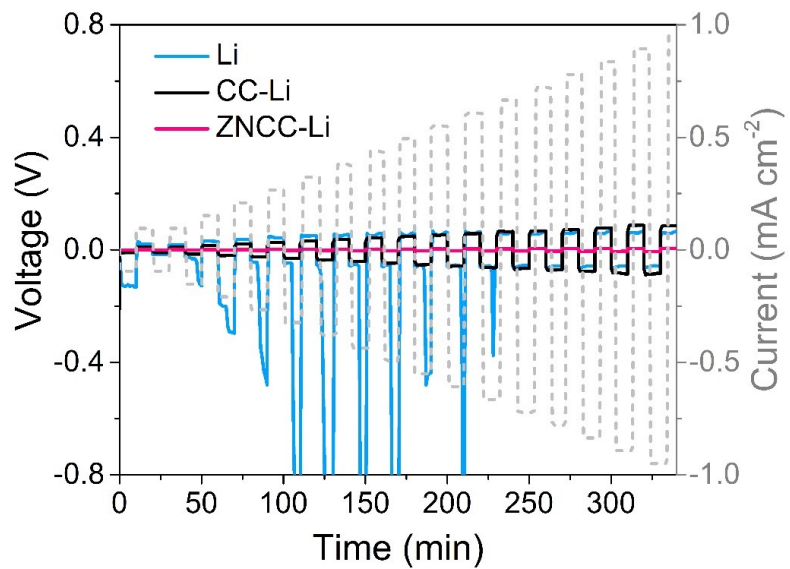
Fig. S15 Voltage profiles of Li, CC-Li and ZNCC-Li at gradual increased current density.
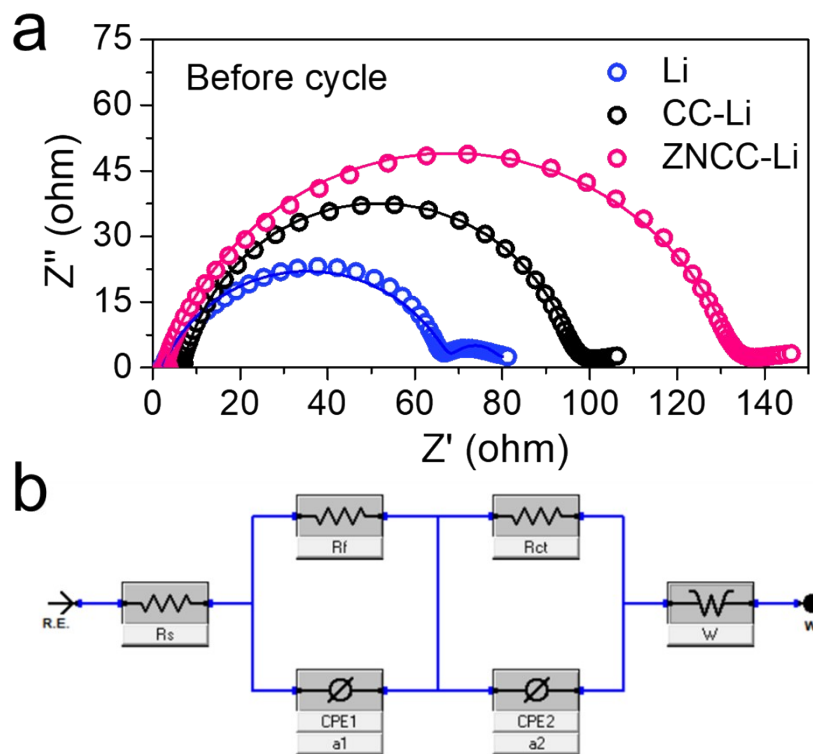
Fig. S16 (a) EIS spectra before cycling at gradual increased current density. (b)

Equivalent circuit used to fit the impedance data.
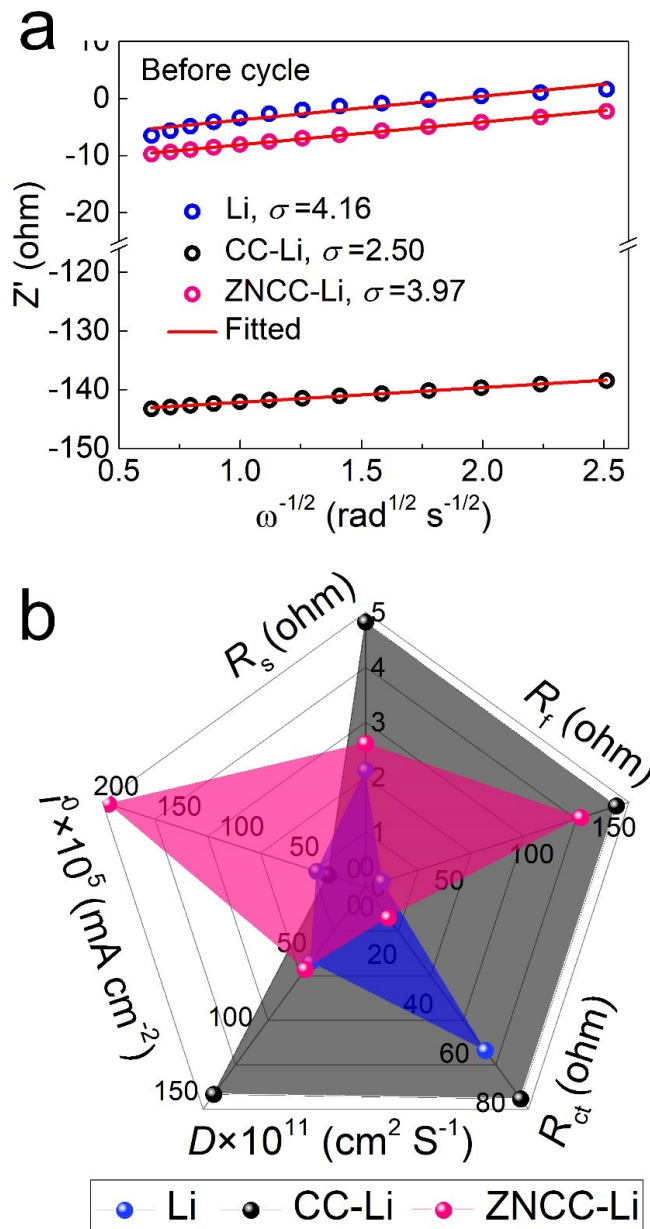
Fig. S17 (a) Calculation of Warburg factor σ before cycling at gradual increased current density. (b) Radar figure of fitted electrochemical parameters of Li, CC-Li and ZNCC-Li.

Table S1 Electrochemical parameters calculated from EIS spectra before cycling at gradual increased current density.

Sample	R_s (Ω)	R_f (Ω)	R_{ct} (Ω)	σ (Ω cm^2 s$^{1/2}$)	D (cm^2 S^{-1})	i^0 (mA cm^{-2})
Li	2.126	10.28	66.27	4.16	5.07×10^{-10}	3.88×10^{-4}
CC-Li	4.825	152.5	85.85	2.50	1.40×10^{-9}	2.99×10^{-4}
ZNCC-Li	2.613	130.8	12.51	3.97	5.57×10^{-10}	2.05×10^{-3}
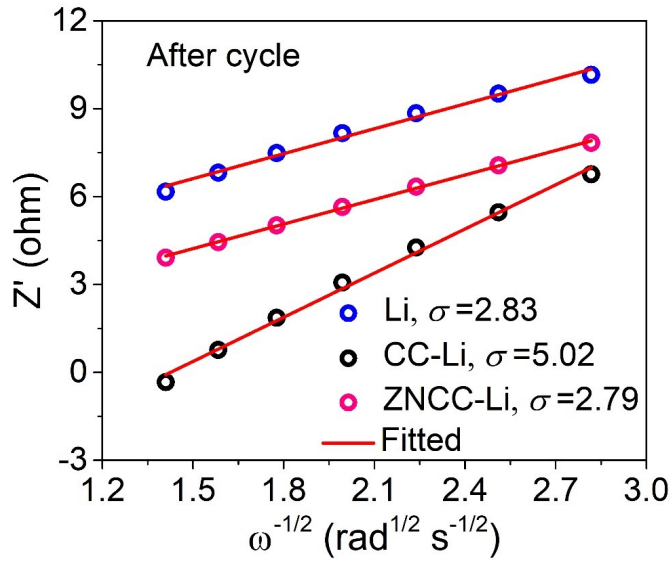
Fig. S18 Calculation of Warburg factor σ after cycling at gradual increased current

density.

Table S2 Electrochemical parameters calculated from EIS spectra after cycling at gradual increased current density.

Sample	R_s (Ω)	R_f (Ω)	R_{ct} (Ω)	σ (Ω cm^2 s$^{1/2}$)	D (cm^2 S^{-1})	i^0 (mA cm^{-2})
Li	1.881	6.292	43.72	2.83	1.10×10^{-9}	5.88×10^{-4}
CC-Li	1.901	9.545	91.99	5.02	3.48×10^{-10}	2.79×10^{-4}
ZNCC-Li	2.814	17.03	29.30	2.79	1.13×10^{-9}	8.77×10^{-4}
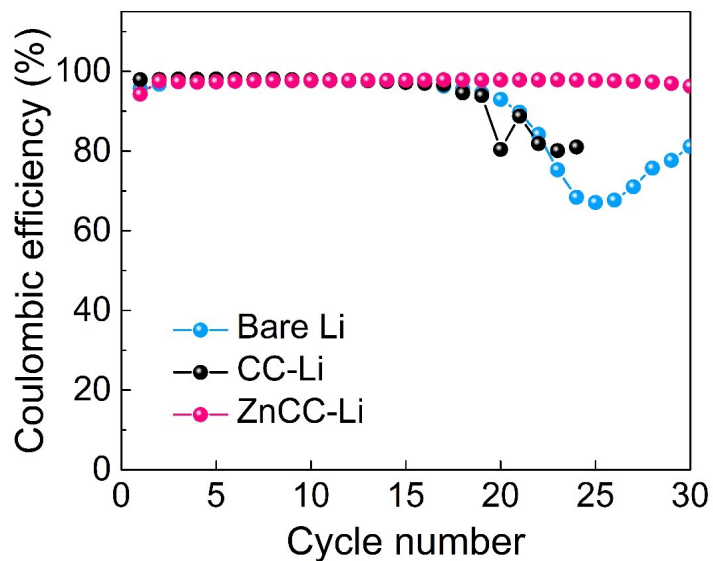
Fig. S19 Coulombic efficiency of Li, CC-Li and ZNCC-Li obtained from Li-Cu cells.
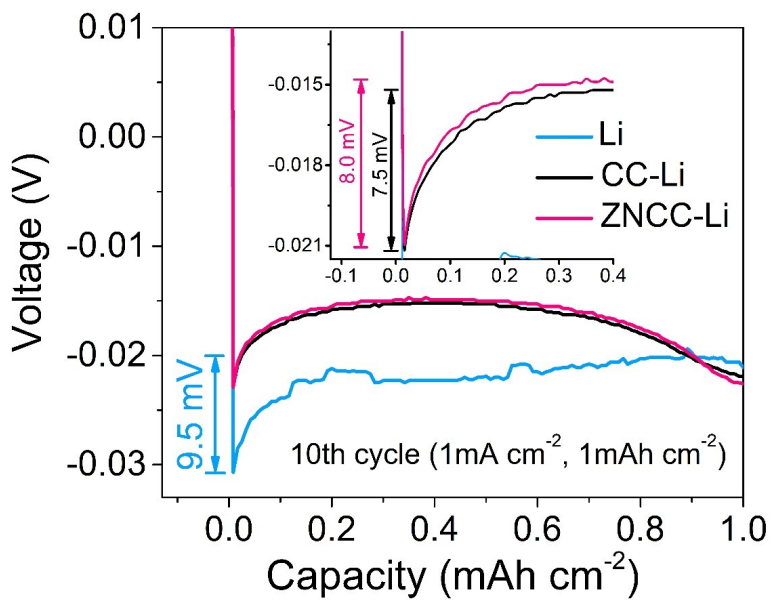
Fig. S20 Voltage profiles of Li-Cu cells during Li nucleation at 10th cycle of bare-Li, CC-Li and ZNCC-Li at 0.5 mA cm⁻² to 1 mAh cm⁻².
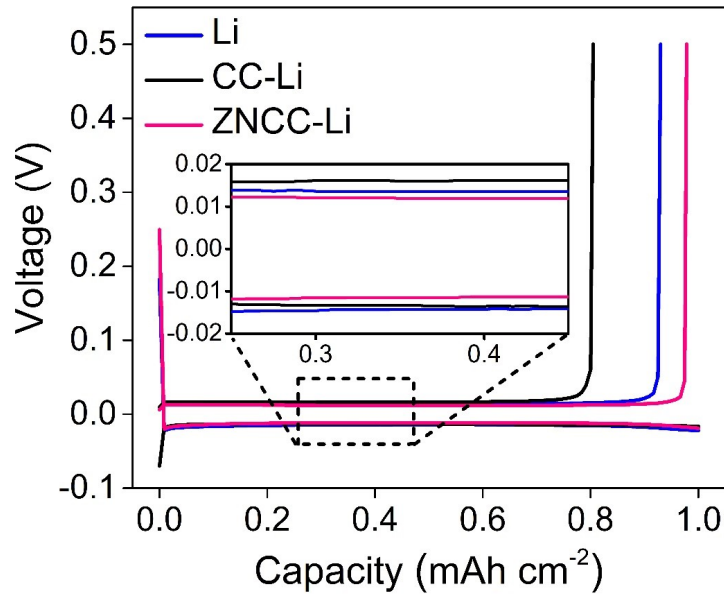
Fig. S21 Charge-discharge profiles of Li-Cu cells at 20th cycle with 0.5 mA cm^{-2} for a total 1 mAh cm^{-2}. ZNCC-Li shows smallest voltage hysteresis.
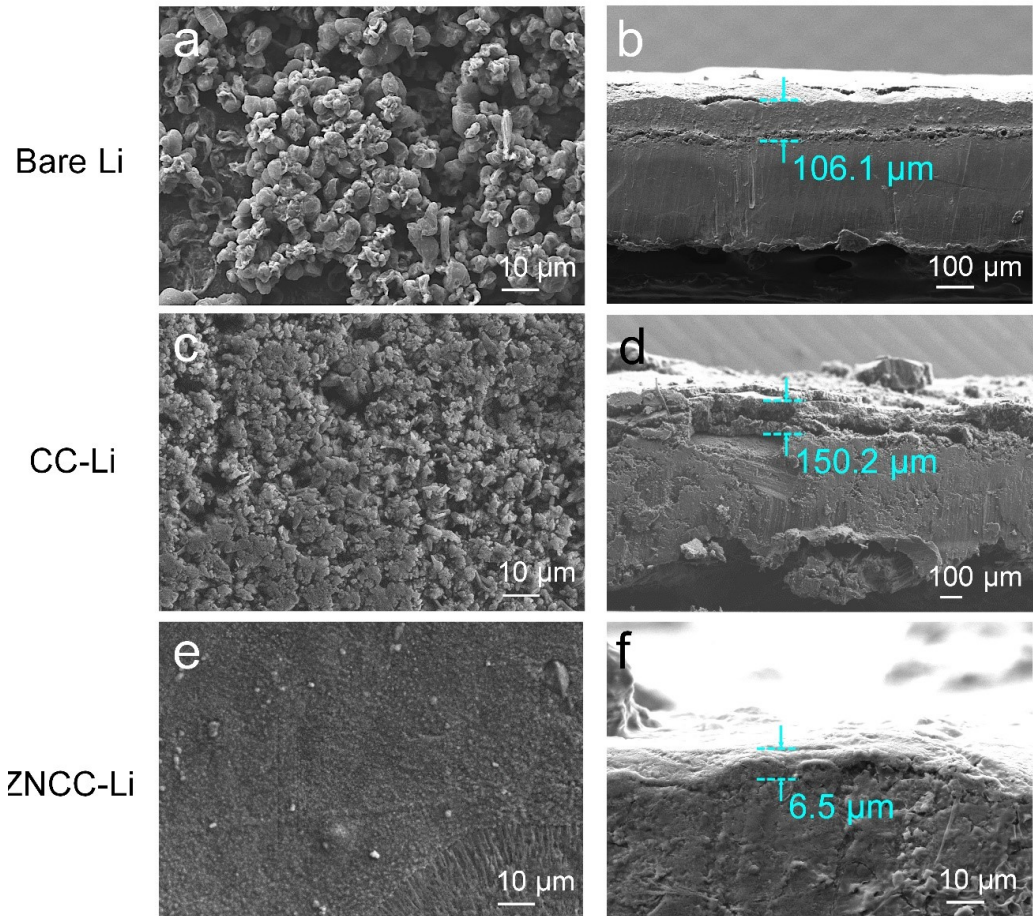
Fig. S22 Top side (a, c, e) and cross-section (b, d, f) SEM images of Li anodes after 500 cycles at 5 mA cm^{-2} to 1 mAh cm^{-2}.
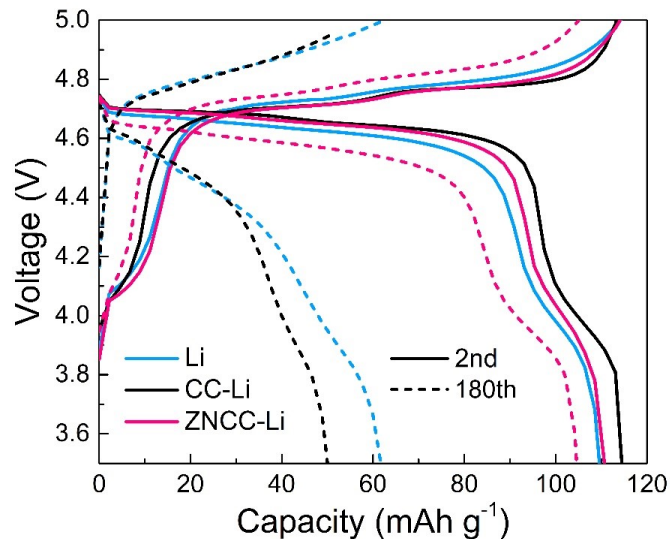
Fig. S23 Voltage profiles of Li, CC-Li and ZNCC-Li at 2nd and 180th cycle.
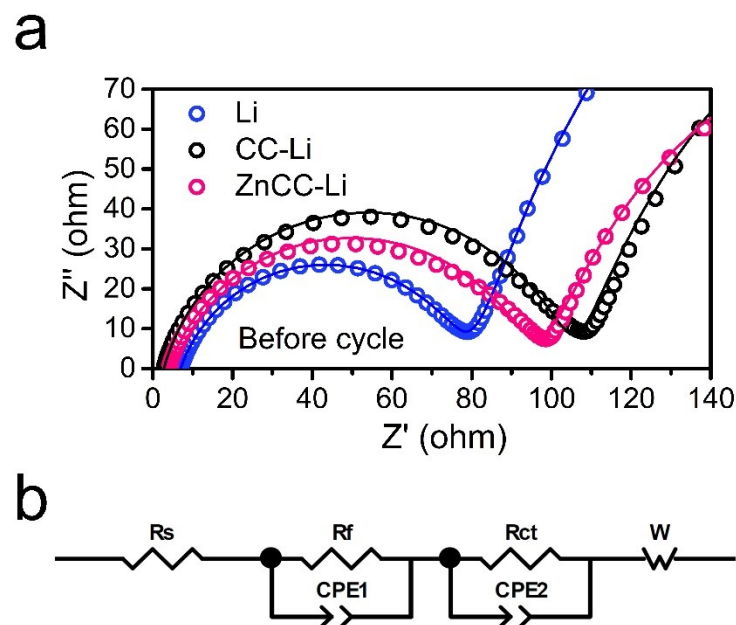
Fig. S24 (a) EIS spectra of full cells before cycling. (b) Equivalent circuit used to fit the

impedance data.
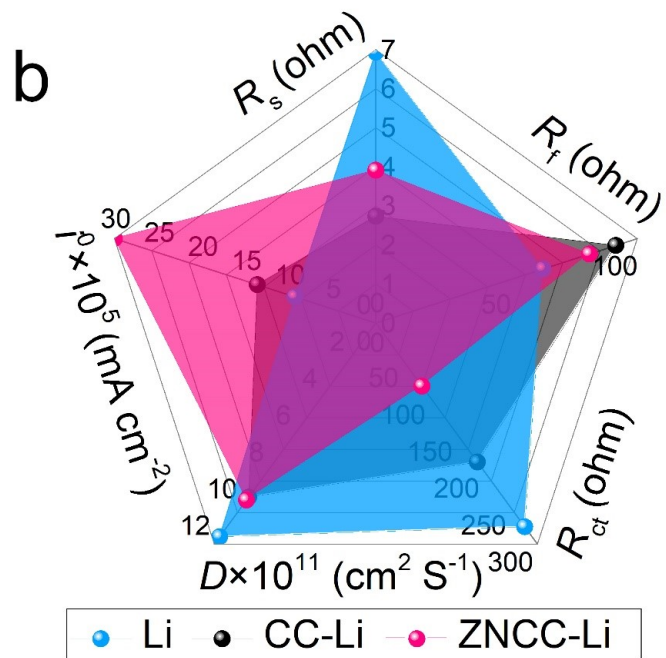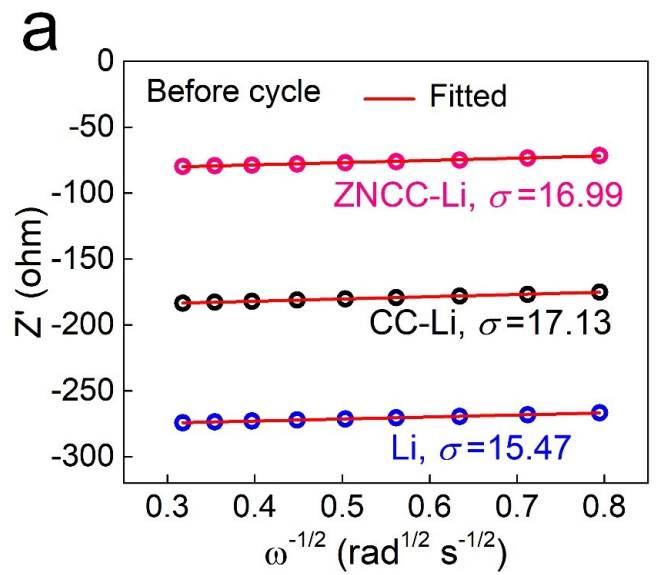
Fig. S25   (a) Calculation of Warburg factor σ of full cells before cycling. (b) Radar

figure of fitted electrochemical parameters of Li, CC-Li and ZNCC-Li.

Table S3 Electrochemical parameters calculated from EIS spectra before cycling.

Sample	R_s (Ω)	R_f (Ω)	R_{ct} (Ω)	σ (Ω cm^2 s$^{1/2}$)	D (cm^2 S^{-1})	i^0 (mA cm^{-2})
Li	6.937	70.35	276.5	15.47	1.16×10^{-10}	9.29×10^{-5}
CC-Li	2.735	101.0	188.7	17.13	9.45×10^{-11}	1.36×10^{-4}
ZNCC-Li	3.914	89.93	85.71	16.99	9.61×10^{-11}	3.00×10^{-4}
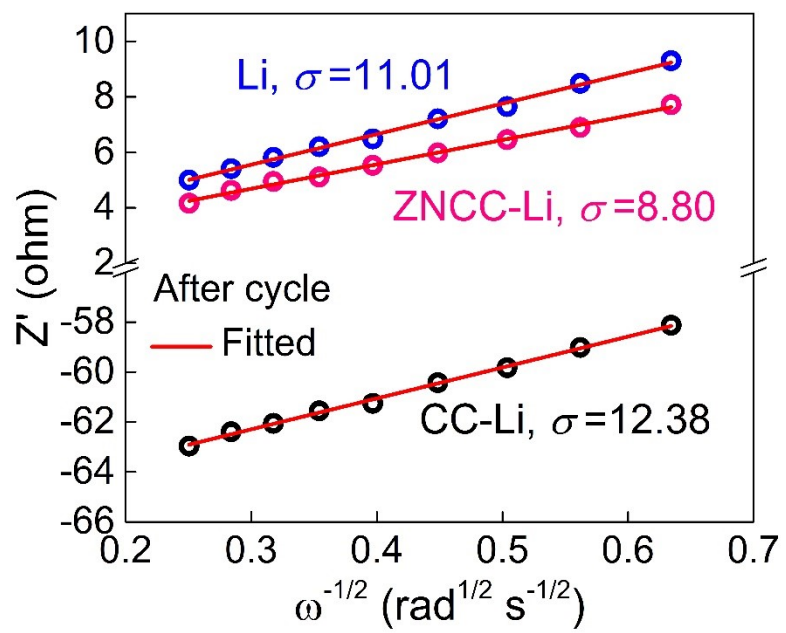
Fig. S26 Calculation of Warburg factor σ of full cells after 180 cycles at 1 C (1 C=133 mAh g^{-1}).
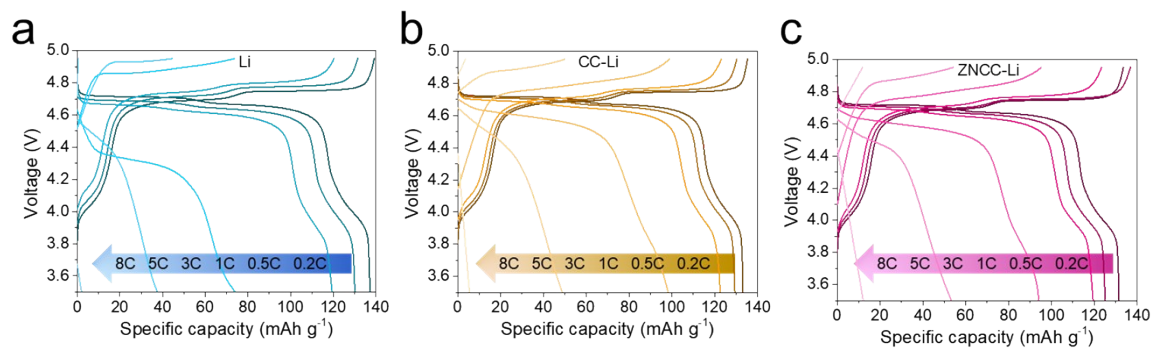
Fig.S27 The charge/discharge curves at different current rates.

Table S4 Electrochemical parameters of full cells calculated from EIS spectra after 180 cycles at 1 C (1 C=133 mAh g^{-1}).

Sample	R_s (Ω)	R_f (Ω)	R_{ct} (Ω)	σ (Ω cm^2 s$^{1/2}$)	D (cm^2 S^{-1})	i^0 (mA cm^{-2})
Li	2.503	12.51	9.424	11.01	2.29×10^{-10}	2.73×10^{-3}
CC-Li	2.226	37.08	58.45	12.38	1.81×10^{-10}	4.40×10^{-4}
ZNCC-Li	2.67×10^{-3}	10.93	7.727	8.80	3.58×10^{-10}	3.32×10^{-3}

Table S5 Li symmetric cells' cycle performance comparison of recently published works of Li metal anode with a host and this work.

Host	Cycle time (h)	Voltage hysteresis (mV)	Current density (mA cm^{-2})	Areal capacity (mAh cm^{-2})	Ref.
NPCC	600	30	3	1	1
g-C$_3$N$_4$@Ni foam	900	15	1	9	2
MG	400	25	5	1	3
CCOF	1000	16	1	1	4
NiF$_x$@NF	1300	~20	1	1	5
V$_2$O$_5$-NF	1600	~18	1	1	6
CCZF	900	~30	1	1	7
Co@N-G	1000	30	1	1	8
CC@CN-Co	800	20	2	1	9
MC@HCNFs	500	~68	2	1	10
NRA-CC	1200	~20	1	1	11
AuLi$_3$@Ni foam	740	~12	0.5	1	12
CFC/Co-NC	100	46	5	1	13
Zn/Cu$_{0.7}$Zn$_{0.3}$/CF	1200	6	2.5	1.5	14
ZNCC	**2300**	**6.4**	**10**	**1**	**This work**

References

1. K. Li, Z. Hu, J. Ma, S. Chen, D. Mu and J. Zhang, *Adv. Mater.*, 2019, **31**, e1902399.
2. Z. Lu, Q. Liang, B. Wang, Y. Tao, Y. Zhao, W. Lv, D. Liu, C. Zhang, Z. Weng, J. Liang, H. Li and Q.-H. Yang, *Adv. Energy Mater.*, 2019, **9**, 1803186.
3. H. Shi, C. J. Zhang, P. Lu, Y. Dong, P. Wen and Z. S. Wu, *ACS Nano*, 2019, **13**, 14308-14318.
4. X.-Y. Yue, W.-W. Wang, Q.-C. Wang, J.-K. Meng, X.-X. Wang, Y. Song, Z.-W. Fu, X.-J. Wu and Y.-N. Zhou, *Energy Stor. Mater.*, 2019, **21**, 180-189.
5. G. Huang, S. Chen, P. Guo, R. Tao, K. Jie, B. Liu, X. Zhang, J. Liang and Y.-C. Cao, *Chem. Eng. J.*, 2020, **395**, 125122.
6. G. Huang, P. Guo, J. Wang, S. Chen, J. Liang, R. Tao, S. Tang, X. Zhang, S. Cheng, Y.-C. Cao and S. Dai, *Chem. Eng. J.*, 2020, **384**, 123313.
7. Y. Li, Y. Wang, Y. Shi, H. Wu, J. Zeng, H. Bu, M. Zhu, C. Xiao, Y. Zhang, G. Gao and S. Ding, *Science Bulletin*, 2020, **65**, 1094-1102.
8. T. S. Wang, X. Liu, X. Zhao, P. He, C. W. Nan and L. Z. Fan, *Adv. Funct. Mater.*, 2020, **30**, 2000786.
9. T. Zhou, J. Shen, Z. Wang, J. Liu, R. Hu, L. Ouyang, Y. Feng, H. Liu, Y. Yu and M. Zhu, *Adv. Funct. Mater.*, 2020, **30**, 1909159.
10. X. Song, H. Wang, H. Wu, J. Zou, F. Zhao, H. Wu and X. Zeng, *Appl. Surf. Sci.*, 2021, **565**, 150589.
11. T. S. Wang, X. Liu, Y. Wang and L. Z. Fan, *Adv. Funct. Mater.*, 2020, **31**, 2001973.
12. X. Ke, Y. Liang, L. Ou, H. Liu, Y. Chen, W. Wu, Y. Cheng, Z. Guo, Y. Lai, P. Liu and Z. Shi, *Energy Stor. Mater.*, 2019, **23**, 547-555.
13. G. Jiang, N. Jiang, N. Zheng, X. Chen, J. Mao, G. Ding, Y. Li, F. Sun and Y. Li, *Energy Stor. Mater.*, 2019, **23**, 181-189.
14. Y. Cheng, X. Ke, Y. Chen, X. Huang, Z. Shi and Z. Guo, *Nano Energy*, 2019, **63**, 103854.